ACS Catalysis

RESEARCH ARTICLE

pubs.acs.org/acscatalysis

Participation of Oligovanadates in Alkane Oxidation with H_2O_2 Catalyzed by Vanadate Anion in Acidified Acetonitrile: Kinetic and DFT Studies

Marina V. Kirillova,[†] Maxim L. Kuznetsov,[*,†] Yuriy N. Kozlov,[‡] Lidia S. Shul'pina,[§] Alex Kitaygorodskiy,[⊥] Armando J. L. Pombeiro,[†] and Georgiy B. Shul'pin[*,‡]

[†]Centro de Química Estrutural, Complexo I, Instituto Superior Técnico, Universidade Técnica de Lisboa, Avenida Rovisco Pais, 1049-001 Lisbon, Portugal

[‡]Semenov Institute of Chemical Physics, Russian Academy of Science, Ulitsa Kosigina, dom 4, 119991 Moscow, Russia

[§]Nesmeyanov Institute of Organoelement Compounds, Russian Academy of Sciences, Ulitsa Vavilova, dom 28, Moscow 119991, Russia

[⊥]Clemson University, Clemson, South Carolina 29634-0973, United States

Supporting Information

ABSTRACT: The efficient oxidation of alkanes (cyclohexane, *n*-heptane, methylcyclohexane, isooctane, *cis*- and *trans*-1,2-dimethylcyclohexane) to the corresponding alkyl hydroperoxides with the system $(n\text{-}Bu_4N)[VO_3]/H_2O_2$/trifluoroacetic acid/MeCN−H_2O was investigated in detail by ^{51}V NMR, kinetic and theoretical methods. It has been established on the basis of the selectivity parameters in the oxidation of linear and branched alkanes and the kinetic peculiarities of the cyclohexane oxidation that the reaction mechanism includes the formation of HO• radicals. The presence of acid (TFA) is the crucial factor in this process, since in the neutral medium, monovanadate is inactive as a catalyst. The role of the acid is explained by the formation of oligovanadates in acidic medium, which exhibit higher catalytic activity compared with the monovanadate. The theoretical DFT calculations that used an oxodivanadate as a model of the catalytically active species revealed that the key factor of the higher activity of oligovanadates is the modification of the reaction mechanism upon the introduction of the second vanadium fragment into the catalyst molecule. As a result, the model divanadate catalyst is more active, by 4.2 kcal/mol (i.e., by a factor of ca. 1200), than the simple monovanadate species. Less energetically demanding routes (H-transfer to the oxo-ligand in the rate-limiting step) are opened for the di(poly)vanadate catalysts but not accessible for the monovanadate catalyst. Moreover, the second vanadium fragment plays the role of a stabilizer of key transition states due to the formation of 6-membered cyclic structures.

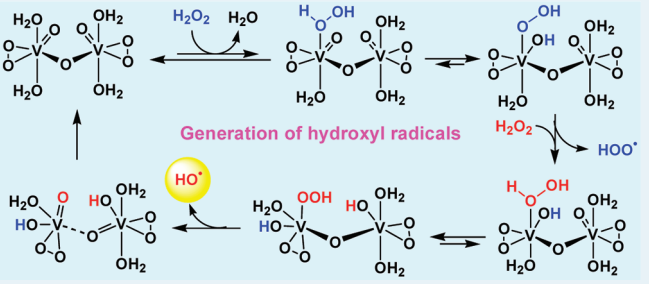

KEYWORDS: alkanes, DFT calculations, homogeneous catalysis, hydrogen peroxide, oligovanadates, oxidation, polyvanadates, reaction mechanism, vanadium

INTRODUCTION

Oxo complexes of vanadium[1−3] and their peroxo derivatives[4−7] play an important role in living nature.[8−14] Enzymes bearing vanadium ions are able to oxidize organic compounds; for example, vanadium-containing haloperoxidases catalyze the halogenation of organic species in the presence of hydrogen peroxide and a halide anion.[15−22] Vanadium compounds are also known as catalysts for various oxidations of organic substrates,[23−32] particularly, saturated,[33−39] aromatic,[40−46] and olefinic[47−49] hydrocarbons by hydrogen peroxide and some other peroxides (for example, $S_2O_8^{2-}$ anion[50] and TBHP).[51] Among these processes, the oxidation of alkanes is of special interest because, on one hand, hydrocarbons of this type are cheap and abundant in nature and, hence, important as precursors for the synthesis of various useful products, but on the other hand, their activation is a rather difficult task.

Previously, it was shown that simple monovanadate VO_3^- efficiently catalyzes the oxidations of alkanes,[52−54] benzene,[52,55] and styrene[56] with H_2O_2 in acetonitrile if pyrazine-2-carboxylic acid (PCA) is added as a cocatalyst in a low concentration. Kinetic studies[53,57] and DFT calculations[58,59] have demonstrated that the mechanism of this process involves the formation of the HO• and HOO• radicals. The former highly reactive radical abstracts[52,60] the hydrogen from alkane RH to give radical R• which, upon the reaction with O_2, affords the corresponding alkyl hydroperoxide, ROOH. This not very stable compound can be easily transformed into the industrially useful alcohol or ketone (Scheme 1). The presence of PCA is a key factor since, in the

Received: May 6, 2011
Revised: August 5, 2011
Published: September 27, 2011

Scheme 1. Overall Radical Mechanism of the Catalyzed Oxidation of Alkanes by H_2O_2

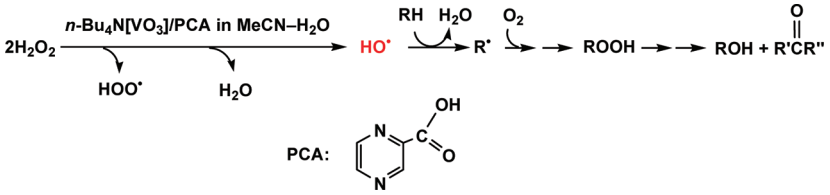

absence of this additive, monovanadate VO_3^- does not exhibit any catalytic activity *in neutral medium* in acetonitrile toward the oxidation of alkanes. DFT calculations have demonstrated that the activation barrier of the HO• formation in the presence of PCA is 9.6 kcal/mol lower than that in the absence of PCA. It was revealed that anion pca^- derived from PCA plays a role of the chelating agent, forming the V−pca complexes and stabilizes a transition state of the rate-limiting step, decreasing the activation barrier compared with the PCA-free system.[59]

At the same time, not only the chelating properties of the pca^- anion but also the acidity of the medium determine the catalytic activity of the vanadate in acetonitrile solution. Indeed, the presence of an acid other than PCA (perchloric,[53,61] nitric,[62] sulfuric,[63] or oxalic[63] acid) also accelerates the reaction and makes possible the alkane oxidations in acetonitrile or water without any N,O-chelating additives. The acidity of the reaction mixture and the protonation of V catalysts (haloperoxidase models) were found to be crucial also in reactions of the oxidation of halides and organic sulfides;[64−67] however, the mechanism proposed for these processes is very different from that established for the oxidation of alkanes. In the latter case, the reasons and driving forces of such interesting pH-dependent behavior of V-catalysts are not known yet. It should be noted that the majority of the haloperoxidase/dialkyl sulfide oxidation reactions are catalyzed by metal complexes with high-affinity chelating ligands, whereas the present studies are focusing on "simple" vanadates. The catalysts of the first group inhibit the dimerization/oligomerization reactions seen in this study. Thus, the main goals of this work are to investigate in detail by both experimental kinetic and theoretical methods why the acidification affects so significantly the oxidation of alkanes, what are the driving forces of this effect, and how does the presence of acid modify the reaction mechanism.

As a starting hypothesis of this work, we proposed that the acid addition to the vanadate solution in acetonitrile promotes the formation of oligovanadates that exhibit higher catalytic activity toward the generation of the HO• radicals and, hence, of the oxidation of alkanes, compared with the monovanadate. To verify this hypothesis, an extended experimental and theoretical mechanistic study of the alkane (cyclohexane) oxidation in the system vanadate/H_2O_2/acid/MeCN−H_2O (acid = trifluoroacetic acid, TFA) was carried out, and the reactivity of the mono- and divanadate catalysts was compared.

This article consists of three main parts. In the first part, the composition of vanadate solutions in the absence and in the presence of TFA was studied by ^{51}V NMR. The second part is devoted to the experimental kinetic investigation of alkane oxidation by the vanadate/H_2O_2/TFA/MeCN−H_2O system. In the third part, plausible mechanisms of the HO• and HOO• radicals' generation catalyzed by divanadate and monovanadate (for comparison) complexes in the presence of H_2O_2 are discussed, and the reasons for the acceleration of the HO• formation in acidified acetonitrile are analyzed on the basis of theoretical DFT calculations.

Chart 1

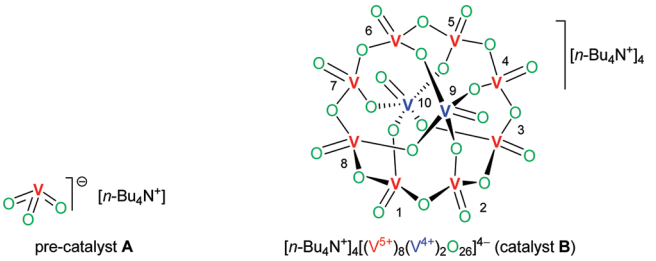

RESULTS AND DISCUSSION

In this work, we have found that the salt $[n\text{-}Bu_4N][VO_3]$ (**A**) (Chart 1) catalyzes the oxidation of alkanes with H_2O_2 in acetonitrile if trifluoroacetic acid (TFA) in low concentration is added. Compound **A**, which is the simple vanadate, was used in the form of the *n*-tetrabutylammonium salt soluble in acetonitrile (for the preparation, see ref 53). No oxidation occurs in the absence of TFA. We also studied a second complex, $[n\text{-}Bu_4N]_4[V_{10}O_{26}]$ (compound **B**; for the preparation, see refs 68−70), which is an oligovanadate containing a cycle consisting of eight V(V) ions (shown in red) and two V(IV) (in blue) situated under and over the plane of the cycle. Tetra-*n*-butylammonium cations were used in this charged compound. Complex **B** catalyzes the alkane oxidation with H_2O_2 in the absence of any acid.

Studies by ^{51}V NMR, kinetic, and DFT methods were carried out to evaluate the oxidation mechanism. The obtained results are given below.

Formation of Oligovanadates in Acidified Acetonitrile. ^{51}V NMR spectra of vanadium species present in a solution of **A** dramatically depend on the batch of acetonitrile used to prepare the sample (compare Figure S1a and b of the Supporting Information); however, the differences between acetonitrile batches practically disappear in the presence of H_2O_2, and their significance for interpreting the catalytic data is unlikely. Spectra S1 demonstrate that the simple monomeric vanadate **A** when dissolved in MeCN is transformed into a few new species that may be complexes with water, MeCN, or both. In the presence of TFA, a large number of signals of comparable intensity appear between −490 and −610 ppm (Figure S2 of the Supporting Information). This region of chemical shifts is typical for oxovanadate oligomers,[71] and one can assume that several different oligomers in the presence of TFA coexist simultaneously at comparable concentrations. Upon addition of excess of H_2O_2, these

dx.doi.org/10.1021/cs200237m |ACS Catal. 2011, 1, 1511−1520

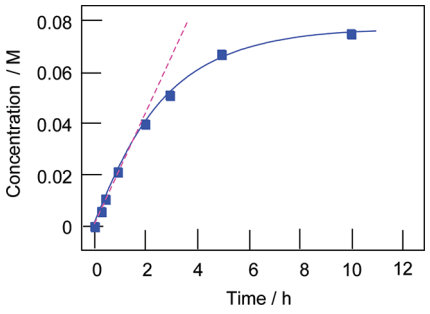

Figure 1. Accumulation of oxygenates (predominantly cyclohexyl hydroperoxide) with time in cyclohexane oxidation with H_2O_2 catalyzed by complex **A** in the presence of TFA in acetonitrile. Conditions: $[\mathbf{A}]_0 = 1 \times 10^{-4}$ M, [TFA] = 8.2×10^{-4} M, $[\text{cyclohexane}]_0 = 0.91$ M, $[H_2O_2]_0 = 1.1$ M, and $[H_2O]_{total} = 2.2$ M, 50 °C.

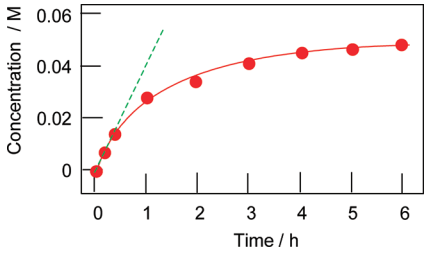

Figure 2. Accumulation of oxygenates (predominantly cyclohexyl hydroperoxide) with time in cyclohexane oxidation with H_2O_2 catalyzed by complex **B** in acetonitrile. Conditions: $[\mathbf{B}]_0 = 1 \times 10^{-4}$ M, $[\text{cyclohexane}]_0 = 0.91$ M, $[H_2O_2]_0 = 1.1$ M, and $[H_2O]_{total} = 2.2$ M, 50 °C.

oligomers turn into mono- and diperoxovanadate complexes[71] (Figures S3 and S4 of the Supporting Information).

The spectrum of the **A**/TFA/H_2O_2 system can be conditionally divided into three groups of signals: four sharp, high-field signals around −700 ppm that can be assigned to the diperoxo complexes;[71−75] a sharp, low-field signal at −437 ppm; and a group of broad signals around −600 ppm that belong to the monoperoxo species.[74,76,77] With increasing concentration of peroxide (and water), the group of medium-field signals moves upfield, and one broad signal starts dominating the spectrum. It is interesting that the relative amount of mono- and diperoxo species remains practically the same at high concentrations of hydrogen peroxide. The spectrum of the **B**/H_2O_2 solution resembles that of **A**/TFA/H_2O_2, and therefore, we can conclude that the compositions of vanadium species in these two systems are very close. For additional details, see the Supporting Information.

Oxidation of Alkanes. Compounds **A** and **B** catalyze the efficient oxidation of alkanes with H_2O_2 in acetonitrile. The oxygenation of alkanes usually gives rise to the formation of the corresponding alkyl hydroperoxides as the main products as well as minor amounts of alcohols and ketones. To estimate real concentrations of alkyl hydroperoxides, ketones (aldehydes), and alcohols present in the reaction mixture, we used a simple method[25,26,78,79] developed earlier by some of us: samples of the reaction solutions were analyzed twice by GC, before and after addition of PPh_3. In our kinetic studies of the cyclohexane oxidation for precise determination of oxygenate concentrations, only data obtained after reduction of the reaction sample with PPh_3 were usually used, taking into account that the original

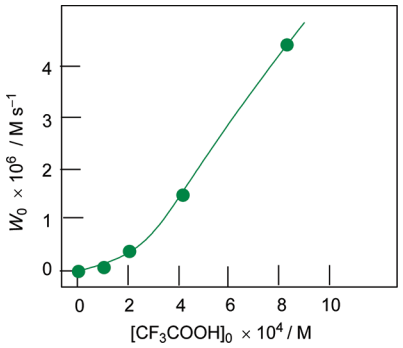

Figure 3. Oxidation of cyclohexane (0.46 M) with hydrogen peroxide (50% aqueous; 2.2 M; total content of water in the reaction mixture, 4.2 M) catalyzed by compound **A** (1×10^{-4} M) in the presence of TFA in MeCN at 50 °C. Dependence of the initial rate of oxygenate formation, W_0, on concentration of added TFA is shown. Concentrations of cyclohexanone and cyclohexanol were determined after reduction of the aliquots with solid PPh_3.

reaction mixture typically contained the three products cyclohexyl hydroperoxide (as a primary product), cyclohexanone, and cyclohexanol.

Accumulation of products in the cyclohexane oxidation catalyzed by **A** and **B** are shown in Figures 1 and 2, respectively. It should be noted that catalyst **A** is active only in the presence of TFA (Figure 3), whereas compound **B** catalyzes this reaction in the absence of TFA. Figure 3 clearly demonstratres that monovanadate does not exhibit catalytic activity, and only in the presence of TFA does the alkane oxidation occur. In the absence of added acids, the vanadium ion exists predominantly in the form of monovanadate (see Section 1). It can therefore be concluded that monovanadate in the absence of added TFA has very low catalytic activity. The great increase in the oxidation rate when an acid is added is not due to the changes in the catalytic activity of the starting monovanadate in the presence of protons. On the other hand, it is well-known[71−75] that addition of an acid leads to the aggregation of monovanadate species and formation of oligovanadates (see Section 1). As DFT calculations (see Section 3) demonstrate, the catalytic activity of divanadate is many times higher in comparison with that of monovanadate, even in the presence of an acid. The second vanadium ion in the divanadate may facilitate proton transfer from coordinated hydrogen peroxide to the oxo group of the divanadate. Taking this into account, we can expect that other highly aggregated oligovanadate species have noticeably higher catalytic activity in comparison with the monovanadate.

Equilibrium constants of the aggregation processes of vanadium ions in studied solutions are unknown, and hence, we were unable to calculate the distribution of vanadium ions for the various oligovandate species. Addition of H_2O_2 may lead to partial disaggregation of oligovanadates, but equilibrium constants for these transformations are also unknown. This is why we cannot interpret in detail the dependences measured by us of the initial oxidation rate, W_0, on initial concentrations of the starting monovanadate **A** (Figure S9 of the Supporting Information) and oligovanadate **B** (Figure S10 of the Supporting Information) and on concentrations of hydrogen peroxide (Figures S11 and S12 of the Supporting Information). All these dependences are straight lines. It should be noted that since the oxidation rate depends on the concentration of water in the solution (the higher the

dx.doi.org/10.1021/cs200237m |*ACS Catal.* 2011, 1, 1511–1520

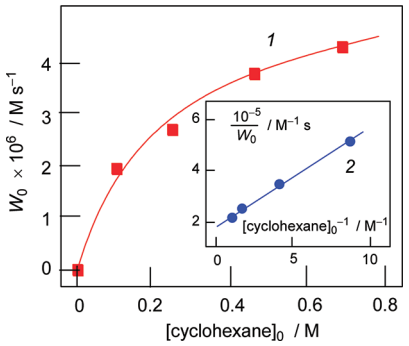

Figure 4. Oxidation of cyclohexane with hydrogen peroxide (50% aqueous; 2.2 M; the total content of water in the reaction mixture was 4.2 M) catalyzed by compound **A** (1×10^{-4} M) in the presence of TFA (8.2×10^{-4} M) in MeCN at 50 °C. Dependence of the initial rate of oxygenate formation, W_0, on the initial concentration of cyclohexane is shown (curve 1). Linearization of curve 1 in coordinates $[\text{cyclohexane}]_0^{-1}$,$W_0$ is presented in line 2. Concentrations of cyclohexanone and cyclohexanol were determined after reduction of the aliquots with solid PPh_3.

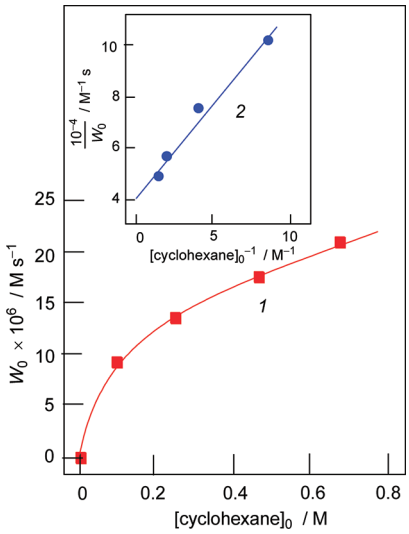

Figure 5. Oxidation of cyclohexane with hydrogen peroxide (50% aqueous; 2.2 M; the total content of water in the reaction mixture was 4.2 M) catalyzed by compound **B** (1×10^{-4} M) in MeCN at 50 °C. Dependence of the initial rate of oxygenate formation, W_0, on initial concentration of cyclohexane is shown (curve 1). Linearization of curve 1 in coordinates $[\text{cyclohexane}]_0^{-1}$,$W_0$ is presented in line 2. Concentrations of cyclohexanone and cyclohexanol were determined after reduction of the aliquots with solid PPh_3.

water concentration, the lower the reaction rate, in agreement with previous results,[53,59] see Figure S13 of the Supporting Information), the concentration of water was maintained constant in the experiments shown in Figures S11 and S12.

For the same reason, we used TFA as an acid that does not contain water in any noticeable concentration. The change in concentrations of catalytically active peroxo complexes depends also on the change in the distribution of vanadium ions among the various oligovanadate forms. We might assume that the concentrations of oligovanadates do not depend on the total concentration of vanadium in the solution, but the probability of this situation is very low. Alternatively, we can propose that the different concentrations of oligovanadate species (x_i) are compensated by their different reactivities (constants k_i). As a result, the measured reaction rate is proportional to the total vanadium concentration. Indeed, in this case, the initial reaction rate is

$$W_0 = \sum_i k_i x_i$$

where i is different reactive forms of aggregated vanadium ions. Let us transform this equation:

$$W_0 = \sum_i k_i x_i = \sum_i k_i \frac{x_i}{[\mathbf{A}]_0}[\mathbf{A}]_0 = \left(\sum_i k_i \frac{x_i}{[\mathbf{A}]_0}\right)[\mathbf{A}]_0$$

If the following condition is obeyed,

$$\sum_i k_i \frac{x_i}{[\mathbf{A}]_0} = \text{const}$$

the initial oxidation rate, W_0, is proportional to the total concentration of vanadium in the solution; that is, $[\mathbf{A}]_0$. This conclusion is in good agreement with the experimentally found dependence that is presented in Figure S9.

Compound **B** containing 10 vanadium ions in the MeCN/H_2O solution in the absence of an acid dissociates, giving a mixture of oligovanadates (see Section 1). This explains the high catalytic activity of compound **B** in the absence of an acid. The specific activity of catalyst **B** calculated as the ratio of the reaction rate to the total number of vanadium ions in the solution is approximately 3.5 times lower than the specific activity of monovanadate **A** in the presence of TFA. It should be noted that the apparent activation energies of oxidations catalyzed by **A** and **B** are very close. Indeed, kinetic data of oxidations at different temperatures (Figure S14) allowed us to calculate the apparent activation energies as 22 ± 2 kcal/mol.

The selectivity parameters obtained in the oxidation of linear and branched alkanes (see the Supporting Information, Table S2) catalyzed by both **A** + TFA and **B** show that in these cases, the oxidizing species is the hydroxyl radical. Additional support for this statement was obtained from kinetic data presented in Figures 4 and 5. Indeed, the mode of dependency of W_0 on initial concentration of the oxidized substrate cyclohexane (that is, asymptotic approaching W_0 to a plateau with growing $[\text{cyclohexane}]_0$) indicates that there is a competitive interaction between the cyclohexane or acetonitrile and the oxidizing species, X. In the interval $[\text{cyclohexane}]_0 \approx 0-0.2$ M, the W_0 value increases roughly proportionally to the initial cyclohexane concentration. At high concentrations of cyclohexane (>0.5 M), the W_0 value does not depend so much on its concentration (approaching to a plateau) because in this case, the main portion of species X generated in the oxidizing systems is accepted by the hydrocarbon. Assuming that in the absence of the cyclohexane the main reaction of the X consumption is the interaction (which leads to the formation of a variety of products[80,81]) between X and the solvent MeCN, we can propose the kinetic scheme of the concurrent oxidation of the alkane, RH, with the following rate-limiting steps:

$$\text{X} + \text{MeCN} \rightarrow \rightarrow \text{products} \quad k_a \qquad \text{(a)}$$

$$\text{X} + \text{RH} \rightarrow \rightarrow \text{ROOH} \quad k_b \qquad \text{(b)}$$

Assuming that the rate of X generation by the catalytic system is W_i, we obtain (for details, see Supporting Information) in the

dx.doi.org/10.1021/cs200237m |ACS Catal. 2011, 1, 1511–1520

Scheme 2. Simplified Mechanism of Radical Generation Catalyzed by Complex $[V(=O)_2(pca)(S)]$

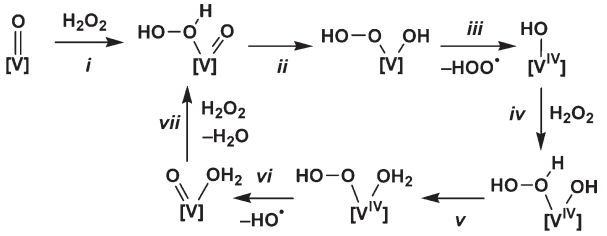

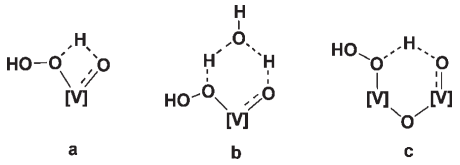

Figure 6. Types of transition states for H transfers.

quasi-stationary approximation for [X] the following equation for the RH oxidation rate:

$$-\frac{d[RH]}{dt} = \frac{d[ROOH]}{dt} = \frac{W_i}{1 + \frac{k_a[MeCN]}{k_b[RH]}} \qquad (c)$$

In accord with eq c, the reciprocal RH oxidation rate should be linearly dependent on the reciprocal concentration of RH:

$$\left(-\frac{d[RH]}{dt}\right)^{-1} = \frac{1}{W_i}\left(1 + \frac{k_a[MeCN]}{k_b[RH]}\right) \qquad (d)$$

Equation d satisfactorily describes the experimental data for both **A** + TFA and **B** (see linear anamorphoses 2 in Figures 4 and 5), meaning that our kinetic scheme is in agreement with the kinetic data. Calculated from the experimental parameters, the ratio of rate constants k_a/k_b for catalyst **A** + TFA is 0.011. The same ratio for catalyst **B** is 0.009. Both values are close to the k_a/k_b ratio (0.008) obtained in the photochemical oxidation[82] of cyclohexane with H_2O_2, for which the hydroxyl radical is known to be the oxidant. Thus, we can conclude that the k_a/k_b ratio for oxidations with **A** + TFA and **B** corresponds to the ratio for the interaction of radical $HO^•$ with MeCN and cyclohexane, and therefore, the oxidizing species X in both systems under discussion is the hydroxyl radical.

DFT Study of the Mechanism. The experimental results described previously[53] and in this work (Section 2) suggest that the V-catalyzed oxidations of alkanes in the presence of H_2O_2 occur via a free radical mechanism. The details of this mechanism have been theoretically studied for the V catalyst $[V(=O)_2(pca)(S)]$ where pca is pyrazine-2-carboxylate, S is solvent (MeCN, H_2O).[58,59] The mechanism is based on the generation of the $HO^•$ and $HOO^•$ radicals, the former reacting with alkanes, and includes seven main steps (Scheme 2). It was shown that the second H transfer [step (*v*)] is the rate-limiting step.[59] This and other H transfers are assisted by a water molecule,[59] which allows the formation of six-membered transition states (TS) (type b, Figure 6) instead of the less-stable four-membered TSs (type a, Figure 6). The $HOO^•$ radicals are not sufficiently "strong" to

Scheme 3. Formation of Peroxo-V Complexes from Oxo-V Species

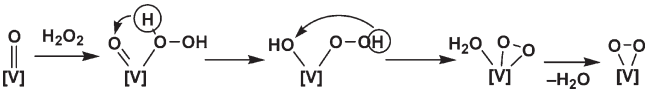

oxidize alkanes; however, they can be involved in a number of side reactions (e.g., $2HOO^• \rightarrow H_2O_2 + O_2$).[53]

The presence of the pca ligand in the catalyst molecule was found to be a crucial factor, since the simple monovanadate VO_3^- in the neutral medium does not catalyze the alkane oxidations. However, as we demonstrate in this work, in the presence of a strong acid (TFA), vanadate becomes active without any additives such as PCA, conceivably due to the formation of oligovanadates (see Sections 1 and 2). We propose here that oligovanadates have a higher catalytic activity than the monovanadate because the second vanadate fragment stabilizes the species involved in the rate-limiting step, playing a role similar to that of pca in the $[V(=O)_2(pca)(S)]$ catalyst. To verify this hypothesis, theoretical mechanistic studies of the $HO^•$ and $HOO^•$ radicals formation with the oxo-μ^1-divanadate $[\{V(=O)_2(H_2O)(S)\}_2O]$ and monovanadate $[V(=O)_2(H_2O)(OH)(S)]$ (for comparison) catalytic systems have been carried out. Only the most plausible pathways are discussed in the text; the less favorable routes are described in the Supporting Information.

Divanadate System. Formation of the Initial H_2O_2 Adduct. It was shown previously for the $[V(=O)_2(pca)(S)]$ system[58,59] that the active form of the catalyst is the oxo−peroxo complex $[V(=O)(OO)(pca)(H_2O_2)]$ rather than the starting dioxo species. Correspondingly, a catalytic cycle for the divanadate should start with the formation of the H_2O_2 complex $[\{V(=O)(OO)(H_2O_2)(H_2O)\}O\{V(=O)(OO)(H_2O_2)_2\}]$ (**1**) from the initial divanadate $[\{V(=O)_2(H_2O)(S)\}_2O]$ (Scheme 3).[57,58]

First H Transfer. Following the formation of the H_2O_2 complex **1**, the next step of the reaction concerns the H transfer from the coordinated H_2O_2 to an oxo ligand to give **2** (Schemes 4 and S2 of the Supporting Information). The water-assisted concerted pathway of this step via formation of transition state TS_{1-2} (Chart 2) is more favorable than the stepwise pathway (see the Supporting Information for details). The calculated activation energy ($\Delta G_s^‡$) of this H transfer is 6.7 kcal/mol (Tables 1 and S3 of the Supporting Information).

Generation of the $HOO^•$ Radical and Formation of the Second H_2O_2 Adducts. Complex **2** may undergo unimolecular elimination of the $HOO^•$ radical and the reduction of the V(1) atom to give **3**. The calculated ΔG_s energy of the reaction **2** → **3** (that is, the adiabatic V−OOH bond energies) is 15.3 kcal/mol, which is slightly higher than the V−OOH bond energy in the complex $[V(OH)(OOH)(OO)(pca)]$ (12.3 kcal/mol[59]). The endoergonic (by 5.8 kcal/mol) addition of another hydrogen peroxide molecule to the tetra-coordinated vanadium site then occurs in **3**, leading to **4**, the latter being in equilibrium with slightly more stable complex **5**.

Second H Transfer. The proton transfer from the coordinated H_2O_2 to the oxo or hydroxo ligand in **4** or **5** affords the hydroperoxo species **6b** or **7b**, whereas the H shifts to the peroxo ligand were previously found to be less favorable.[59] Reactions **4** → **7b** and **5** → **6b** proceed via transition states TS_{4-7b} and TS_{5-6b} involving a water molecule (TSs of type b, Figure 6, Chart 2) whereas the reaction **4** → **6b** includes the formation of TS_{4-6b}

dx.doi.org/10.1021/cs200237m |*ACS Catal.* 2011, 1, 1511–1520

Scheme 4. Catalytic Cycles for the Formation of HOO• and HO• Radicals Based on μ-oxo Complexes[a]

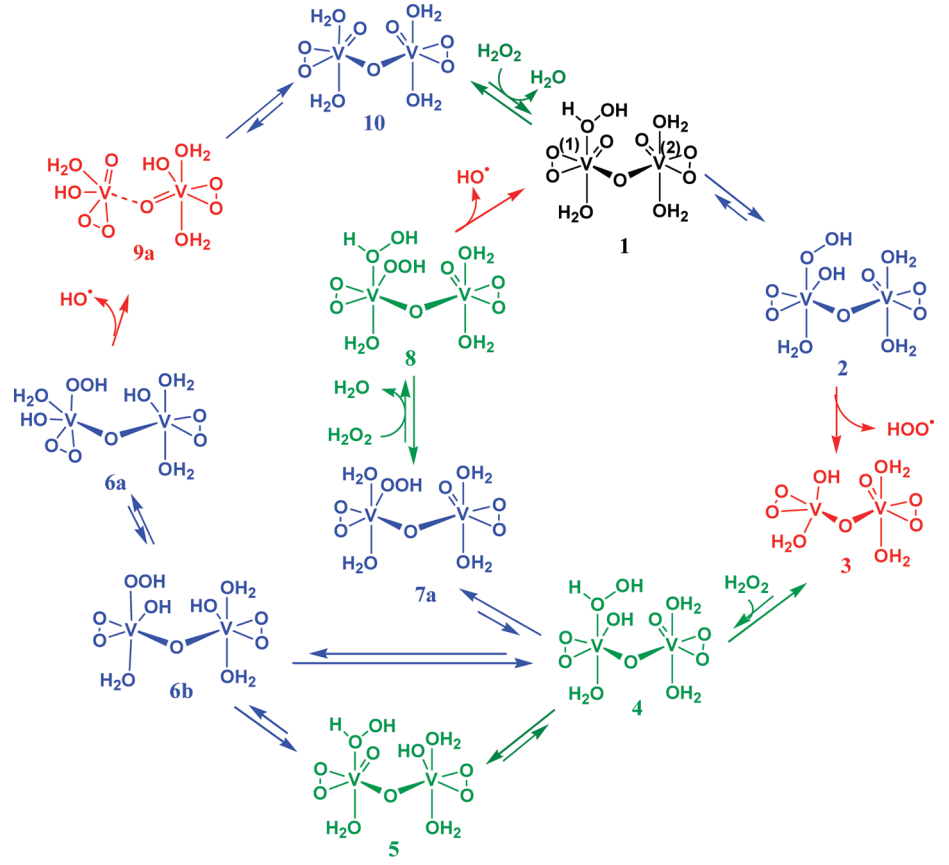

[a] Color code: black, initial catalytic species; blue, H-transfers; red, radical generation; green, formation of H_2O_2 or H_2O adducts. Only the most stable isomers are shown, except complex **6**.

Chart 2

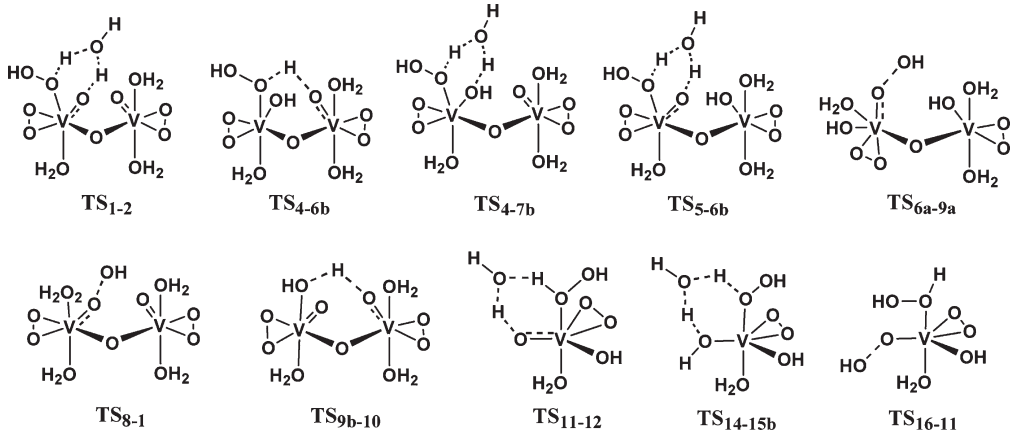

without the assistance of H_2O (TSs of type c). The activation barriers of all these routes are within the range of 6.0−7.5 kcal/mol, and the pathway **5** → **6b** is the most kinetically favorable one (Figure 7). It is worth mentioning that the energy of TS_{5-6b} is lower than the energy of the product **6b**. Such a situation when the energy of TS is lower than that of the reactants or products was described previously for water-assisted H transfers,[59] and it is caused by the formation of a molecular van der Waals complex between the reactant (product) and H_2O. Complexes **6b** and **7b** then undergo an isomerization to the most stable isomers **6a** and **7a**. Finally, the substitution of H_2O for H_2O_2 in **7a** results in the formation of **8**.

Formation of HO• Radical and Catalyst Regeneration. In the last step, the homolysis of the O−O bond in **6a** and **8** via TS_{6a-9a} and TS_{8-1} produces the HO• radicals and oxidizes the V^{IV} atom to the V^{V}. These two reactions have equal and rather

dx.doi.org/10.1021/cs200237m |ACS Catal. 2011, 1, 1511–1520

Table 1. Energetic Characteristics (in kcal/mol) of the Reactions Discussed in the Text

reaction		ΔH_s‡	ΔG_s‡	ΔH_s	ΔG_s
1 → **2**	via TS_{1-2}	−1.1	6.7	−1.6	−2.3
2 → **3** + HOO•				24.9	15.3
3 + H_2O_2 → **4**				−3.7	5.8
4 → **6b**	via TS_{4-6b}	5.1	5.5	6.9	6.0
4 → **7b**	via TS_{4-7b}	−1.7	7.5	0.5	0.0
5 → **6b**	via TS_{5-6b}	−2.1	5.3	8.0	6.8
6b → **6a**				−9.9	−8.4
7b → **7a**				−5.3	−5.0
7a + H_2O_2 → **8** + H_2O				3.6	4.2
6a → **9a** + HO•	via TS_{6a-9a}	6.7	7.2	2.6	−4.2
8 → **1** + HO•	via TS_{8-1}	6.3	7.2	−3.6	−9.6
9a → **9b**				3.7	4.7
9b → **10**	via TS_{9b-10}	−2.4	−1.7	−10.8	−11.9
10 + H_2O_2 → **1** + H_2O				2.7	3.6
11 → **12**	via TS_{11-12}	2.9	11.5	3.6	3.6
12 → **13** + HOO•				24.6	14.8
13 + H_2O_2 → **14**				−5.2	3.8
14 → **15b**	via TS_{14-15b}	−1.1	6.8	2.9	2.4
15b → **15a**				−10.0	−9.5
15a + H_2O_2 → **16** + H_2O				2.1	2.8
16 → **11** + HO•	via TS_{16-11}	5.7	6.3	−3.1	−9.4

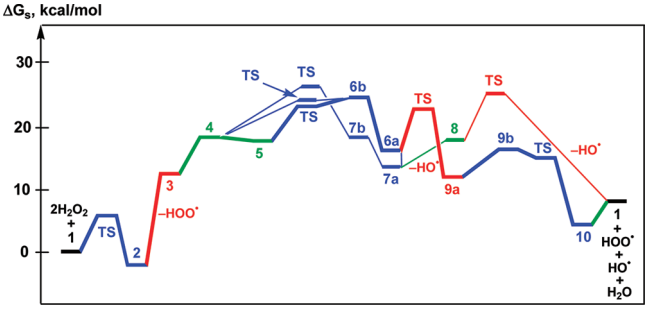

Figure 7. Energy profile of the catalytic cycles based on μ-oxo complexes. For color code, see Scheme 4. The most favorable route is marked by bold lines. Only species bearing vanadium are indicated for the levels (except the first and last levels).

low activation barriers (7.2 kcal/mol). In the case of **8**, the initial active form of the catalyst **1** is directly regenerated and then starts a new catalytic cycle. For the other pathway, the regeneration of **1** takes place via the sequence **6a** → **9** → **10** → **1**.

In addition to the routes based on the monobridged μ-oxo-divanadate system discussed above, other mechanisms involving the formation of di(μ-oxo)-divanadate species may also be realized, and they are described in the Supporting Information. The latter mechanisms are less favorable than the former ones only by 1.3 kcal/mol and, thus, may also be realized to some extent.

Monovanadate System. To compare the reactivity of mono- and divanadate catalysts, the plausible mechanism of the HO• and HOO• formation was also calculated for the simple monovanadate $[V(=O)_2(OH)(H_2O)_2]$ in which the second V fragment is replaced by a proton. The mechanism (Scheme 5, Figure 8) is similar to that described above and includes (i) the formation of the active catalytic form **11**; (ii) the proton transfer

Scheme 5. Catalytic Cycle for the Formation of HOO• and HO• Radicals Based on Monovanadate[a]

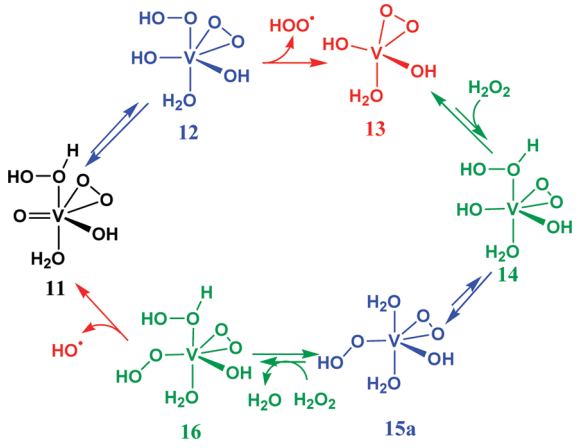

[a] For color code, see Scheme 4. Only the most stable isomers are shown.

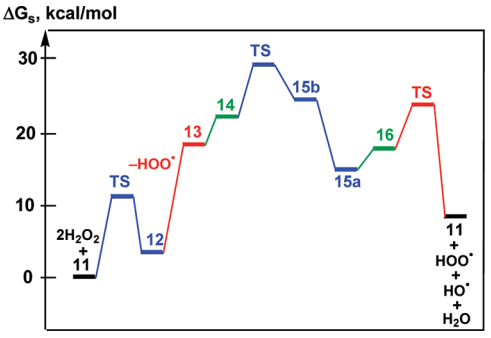

Figure 8. Energy profile of the catalytic cycles based on monovanadate. For color code, see Scheme 4. Only species bearing vanadium are indicated for the levels (except the first and last levels).

from H_2O_2 to the oxo-ligand to give **12** via TS_{11-12} of the type b (Figure 6); (iii) monomolecular generation of HOO• with the ΔG_s value of 14.8 kcal/mol (Table 1) to form **13**; (iv) addition of another H_2O_2 molecule, affording complex **14**; (v) H transfer from H_2O_2 to the OH ligand, leading to **15b**; (vi) isomerization of **15b** to the more stable isomer **15a**; (vii) substitution of H_2O for H_2O_2 in **15a** to give **16**; and (viii) finally, the liberation of the HO• radical via TS_{16-11} and regeneration of the catalyst **11**.

General Discussion of the Mechanisms Based on DFT Calculations. The analysis of the theoretical results described in the previous sections and the Supporting Information allows one to draw several important conclusions. First, the most plausible mechanism of the divanadate catalyzed radical formation includes the sequence of the H_2O_2 addition, H transfer, and HOO• and HO• elimination steps **1** → **2** → **3** → **4** (→ **5**) → **6b** → **6a** → **9a** (+ HO•) → **9b** → **10** → **1**. This mechanism is depicted in Scheme 4, which clearly shows that the most favorable route directly involves the second V fragment of the divanadate catalyst, whereas the route **1** → **2** → **3** → **4** → **7b** → **7a** → **8** → **1** (+ HO•), in which the second V-fragment is not affected, is less favorable.

Second, as may be seen in Figure 7, the rate-limiting step of the overall process is the second H transfer (step **4** (**5**) → **6b**), and the unimolecular HOO• and HO• eliminations are less energetically

dx.doi.org/10.1021/cs200237m |ACS Catal. 2011, 1, 1511–1520

demanding relative to **1**. Third, the presence of the second V fragment in the divanadate molecule provides the possibility of the formation of stable six-membered transition states for the H-transfer processes without involvement of the water molecule (TSs of type c, Figure 6). For some steps (e.g. in the crucial rate limiting step **4** → **6b**), the stabilization of TS by the second V fragment is even greater than by the water molecule.

Fourth, the catalytic activity of the divanadate was found to be obviously higher than that of the monovanadate. Indeed, the calculated apparent Gibbs free energy of activation, $\Delta G_s‡$, relative to **1** of the divanadate catalyzed $HO^•$ formation is 24.8 kcal/mol. This is lower than the activation barrier of the monovanadate-catalyzed process (29.0 kcal/mol). The difference in the activation energies of 4.2 kcal/mol corresponds to the ratio of the rate constants of ∼1200. This ratio is quite sufficient to explain the experimental observations indicating that the monovanadate in neutral medium is not active for the oxidation of alkanes, whereas di- and polyvanadates formed in acidic medium efficiently catalyze this reaction.

Fifth, the higher catalytic activity of the divanadate may be explained as follows: In the case of the monovanadate, the rate-limiting H transfer (**14** → **15**) may occur only to the OH ligand (the H shifts to the peroxo ligand were found to be less favorable).[59] The presence of the second vanadium fragment in the di(poly)vanadates opens the possibility for this H transfer not only to the OH ligand (**4** → **7**) but also to the oxo ligand (**4** (**5**) → **6**). The latter process is less energetically demanding than the former (Figure 7). In addition, the proton migration to the OH ligand itself requires lower energy for the divanadate systems than for the monovanadate (by 2.7 kcal/mol relative to the reactants).

The calculated apparent activation enthalpy, $\Delta H_s‡$, relative to **1** of the $HO^•$ generation catalyzed by divanadate is 26.4 kcal/mol, which is somewhat higher than the experimentally found apparent activation energy of 22 ± 2 kcal/mol (Section 2). However, such a deviation may be considered as reasonable taking into account that only the divanadate complex was used for the DFT calculations, whereas the real catalytic system is much more complicated and bears the mixture of various oligovanadates participating in the reaction.

It is also interesting that the VO_3^-/PCA catalyst exhibits higher catalytic activity compared with the VO_3^-/TFA system. The experimental apparent activation energies for these two catalytic systems are 17 ± 2 kcal/mol[53] and 22 ± 2 kcal/mol (this work, Section 2). The corresponding theoretically calculated $\Delta G_s‡$ values are 19.8 kcal/mol[59] and 24.8 kcal/mol (this work), and they perfectly correlate with the experimental trend.

FINAL REMARKS

The vanadium-catalyzed oxidations of alkanes are very sensitive to the presence of H^+ in the reaction mixture. Simple monovanadate VO_3^- does not exhibit any catalytic activity toward alkanes, but the addition of an acid in a low concentration dramatically accelerates this reaction. In the present work, we investigated in detail the reasons for such interesting and important pH-dependent behavior of the V-catalysts. Our starting hypothesis about the formation of oligovanadates in acidic medium, which are more active toward the oxidation of alkanes than the simple monovanadate was confirmed by both experimental and theoretical methods. ^{51}V NMR and kinetic studies indicate that in the systems VO_3^-/H_2O_2/TFA and $[V_{10}O_{26}]^{4-}/H_2O_2$ in acetonitrile, oligovanadates are responsible for the efficient generation of hydroxyl radicals (key species in the alkane oxidation).

The theoretical calculations reveal that the model divanadate catalyst is more active, by 4.2 kcal/mol (i.e., by a factor of ca. 1200) than the simple monovanadate species. The key factor of the higher activity of the di(oligo)vanadates is the modification of the reaction mechanism upon the introduction of the second vanadium fragment into the catalyst molecule. Namely, additional and less energetically demanding routes (H-transfer *to the oxo ligand* in the rate-limiting step **4**(**5**) → **6b**) are opened for the di(poly)vanadate catalysts but not accessible for the monovanadate one. Moreover, the second vanadium fragment plays the role of a stabilizer of key transition states due to the formation of six-membered dimetalocyclic structures (transition states of type c, Figure 6).

EXPERIMENTAL SECTION

Spectroscopy. ^{51}V NMR spectra were recorded on a Bruker Avance 500 at 131.46 MHz. A typical vanadium spectrum for a 1 mM solution was obtained from the accumulation of 20 000 transients with a 700 ppm spectral window at ∼12 scans/s. Unless it is stated otherwise, spectra were recorded at room temperature (297 K). An exponential line-broadening up to 200 Hz was applied before Fourier transformation. The vanadium chemical shifts are quoted relative to external $VOCl_3$ (0 ppm). Two batches of acetonitrile were used to obtain the NMR spectra. One of them was distilled immediately before the NMR experiments, and the second ("old") was exposed to air for over a month. The differences between acetonitrile batches practically disappear in the presence of H_2O_2. Mainly in NMR and all kinetic studies, we used acetonitrile that was not distilled prior to use.

Oxidation Experiments. Catalysts **A**[53] and **B**[68−70] and cocatalyst TFA were used in the form of stock solutions in acetonitrile. Aliquots of these solutions were added to the reaction mixtures in the oxidations of alkanes. The oxidation reactions were typically carried out in air in thermostatted Pyrex cylindrical vessels with vigorous stirring; total volume of the reaction solution was 5 mL. (**CAUTION**: the combination of air or molecular oxygen and H_2O_2 with organic compounds at elevated temperatures may be explosive!). The reactions were stopped by cooling, and analyzed twice, that is, before and after the addition of an excess of solid PPh_3. This method was developed and used previously by some of us[25,26,78,79] for the analysis of reaction mixtures obtained from various alkane oxidations. Applying this method in the present work for the oxidation of cyclohexane, we demonstrate that the reaction affords predominantly cyclohexyl hydroperoxide as the primary product which slowly decomposes to form cyclohexanol and cyclohexanone. In our kinetic studies for precise determination of oxygenate concentrations, only data obtained after reduction of the reaction sample with PPh_3 were used. A Fisons Instruments GC 8000 series gas chromatograph with a capillary column 30 m × 0.32 mm ×25 μm, DB-WAX (J&W) (helium was the carrier gas; the internal standard was nitromethane) was used. In the kinetic experiments, each oxidation was carried out at least twice, and the average value is shown in the figures. Experimental error was 10%.

Computational Details. The full geometry optimization of all structures and transition states has been carried out at the DFT/HF hybrid level of theory using Becke's three-parameter hybrid exchange functional in combination with the gradient-corrected correlation functional of Lee, Yang, and Parr (B3LYP)[83,84] with

the help of the Gaussian-98 program package.[85] The restricted approximations for the structures with closed electron shells and the unrestricted methods for the structures with open electron shells have been employed. Symmetry operations were not applied for all structures. The geometry optimization was carried out using a relativistic Stuttgart pseudopotential that described 10 core electrons, the appropriate contracted basis set (8s7p6d1f)/[6s5p3d1f][86] for the vanadium atom, and the 6-31G(d) basis set for other atoms. Then single-point calculations were performed on the basis of the found equilibrium geometries using the 6-31+G(d,p) basis set for nonmetal atoms.

The Hessian matrix was calculated analytically for the optimized structures at the B3LYP/6-31G(d) level to prove the location of correct minima (no imaginary frequencies) or saddle points (only one imaginary frequency) and to estimate the thermodynamic parameters, the latter being calculated at 25 °C. The nature of all transition states was investigated by the analysis of vectors associated with the imaginary frequency.

Total energies corrected for solvent effects (E_s) were estimated at the single-point calculations on the basis of gas-phase geometries at the CPCM-B3LYP/6-31+G(d,p)//gas-B3LYP/6-31G(d) level of theory using the polarizable continuum model in the CPCM version[87,88] with CH_3CN as solvent. The entropic term in CH_3CN solution (S_s) was calculated according to the procedure described by Wertz[89] and Cooper and Ziegler[90] (see the Supporting Information). The enthalpies and Gibbs free energies in solution (H_s and G_s) were estimated using the expressions

$$H_s = E_s(\text{6-31+G(d,p)}) + H_g(\text{6-31G(d)}) - E_g(\text{6-31G(d)})$$

$$G_s = H_s - TS_s$$

where E_s, E_g and H_g are the total energies in solution and in gas phase and gas-phase enthalpy calculated at the corresponding level. The electronic structure of some species was analyzed using the natural bond orbital (NBO) partitioning scheme.[91]

■ ASSOCIATED CONTENT

Supporting Information. Additional details of Results and Discussion. Discussion of less favorable reaction mechanisms. Spectra ^{51}V of the vanadates in the presence and absence of TFA. Data on oxidations of linear, branched, and cyclic alkanes: regio-, bond-, and stereoselectivity parameters. Details of kinetic experiments. Computational details. Calculated total energies, enthalpies, entropies, Gibbs free energies. This information is available free of charge via the Internet at http://pubs.acs.org.

■ AUTHOR INFORMATION

Corresponding Author

*E-mails: max@mail.ist.utl.pt (M.L.K.), shulpin@chph.ras.ru (G.B.S.).

■ ACKNOWLEDGMENT

This work was supported by the FCT (Ciência 2007 and PPCDT programs) (Portugal) and the Russian Foundation for Basic Research (Grant 06-03-32344-a). M.V.K. is grateful to the FCT for a postdoctoral fellowship. M.L.K. is grateful to the FCT and IST for a research contract within the Ciência 2007 scientific program. L.S.S. and G.B.S. express their gratitude to the FCT for making it possible for them to stay at the Instituto Superior Técnico, TU Lisbon, as invited scientists and to perform a part of the present work.

■ REFERENCES

(1) Crans, D. C.; Baruah, B.; Ross, A.; Levinger, N. E. *Coord. Chem. Rev.* **2009**, *253*, 2178–2185.
(2) Aureliano, M. *Dalton Trans.* **2009**, 9093–9100.
(3) Hayashi, Y. *Coord. Chem. Rev.* **2011**, *255*, 2270−2280.
(4) Bortolini, O.; Conte, V. *J. Inorg. Biochem.* **2005**, *99*, 1549–1557.
(5) Markov, A. A.; Dolin, S. P.; Moiseeva, N. I.; Gekhman, A. E.; Moiseev, I. I. *Kinet. Katal.* **2009**, *50*, 683–692.
(6) Markov, A. A.; Dolin, S. P.; Moiseeva, N. I.; Gekhman, A. E.; Moiseev, I. I. *Dokl. Akad. Nauk.* **2009**, *426*, 347–350.
(7) Molinari, J. E.; Wachs, I. E. *J. Am. Chem. Soc.* **2010**, *132*, 12559–12561.
(8) Crans, D. C.; Smee, J. J.; Gaidamauskas, E.; Yang, L. *Chem. Rev.* **2004**, *104*, 849–902.
(9) Tracey, A. S.; Willsky, G. R.; Takeuchi, E. S. *Vanadium Chemistry, Biochemistry, Pharmacology and Practical Applications*; CRC Press: Boca Raton, 2007.
(10) Rehder, D. *Bioinorganic Vanadium Chemistry*; Wiley: Chichester, 2008.
(11) Rehder, D. *Org. Biomol. Chem.* **2008**, *6*, 957–964.
(12) Aureliano, M.; Crans, D. C. *J. Inorg. Biochem.* **2009**, *103*, 536–546.
(13) Pereira, M. J.; Carvalho, E.; Eriksson, J. W.; Crans, D. C.; Aureliano, M. *J. Inorg. Biochem.* **2009**, *103*, 1687–1692.
(14) Crans, D. C.; Trujillo, A. M.; Pharazyn, P. S.; Cohen, M. D. *Coord. Chem. Rev.* **2011**, *255*, 2178−2192.
(15) Littlechild, J. *Curr. Opin. Chem. Biol.* **1999**, *3*, 28–34.
(16) Smith, T. S., II.; Pecoraro, V. L. *Inorg. Chem.* **2002**, *41*, 6754–6760.
(17) Butler, A.; Carter-Franklin, J. N. *Nat. Prod. Rep.* **2004**, *21*, 180–188.
(18) Butler, A.; Sandy, M. *Nature* **2009**, *460*, 848–854.
(19) Winter, J. M.; Moore, B. S. *J. Biol. Chem.* **2009**, *284*, 18577–18581.
(20) Walmsley, R. S.; Tshentu, Z. R. *South Afr. J. Chem.* **2010**, *63*, 95–104.
(21) Bernhardt, P.; Okino, T.; Winter, J. M.; Miyanaga, A.; Moore, B. S. *J. Am. Chem. Soc.* **2011**, *133*, 4268–4270.
(22) Werncke, C. G.; Limberg, C.; Knispel, C.; Metzinger, R.; Braun, B. *Chem.—Eur. J.* **2011**, *17*, 2931–2938.
(23) Butler, A.; Clague, M. J.; Meister, G. E. *Chem. Rev.* **1994**, *94*, 625–638.
(24) Shilov, A. E.; Shul'pin, G. B. *Chem. Rev.* **1997**, *97*, 2879–2932.
(25) Shul'pin, G. B. *J. Mol. Catal. A: Chem.* **2002**, *189*, 39–66.
(26) Shul'pin, G. B. *C. R. Chim.* **2003**, *6*, 163–178.
(27) Kustin, K., Costa Pessoa, J., Crans, D. C., Eds.; *Vanadium: the Versatile Metal*; ACS Symposium Series 974; American Chemical Society: Washington, DC, 2007.
(28) Adão, P.; Maurya, M. R.; Kumar, U.; Avecilla, F.; Henriques, R. T.; Kuznetsov, M. L.; Costa Pessoa, J.; Correia, I. *Pure Appl. Chem.* **2009**, *81*, 1279–1296.
(29) Adão, P.; Costa Pessoa, J.; Henriques, R. T.; Kuznetsov, M. L.; Avecilla, F.; Maurya, M. R.; Kumar, U.; Correia, I. *Inorg. Chem.* **2009**, *48*, 3542–3561.
(30) Silva, J. A. L.; Fraústo da Silva, J. J. R.; Pombeiro, A. J. L. *Coord. Chem. Rev.* **2011**, *255*, 2232−2248.
(31) Conte, V.; Floris, B. *Dalton. Trans.* **2011**, *40*, 1419–1436.
(32) Mizuno, N.; Kamata, K. *Coord. Chem. Rev.* **2011**, *255*, 2358−2370.
(33) Gonzalez Cuervo, L.; Kozlov, Y. N.; Süss-Fink, G.; Shul'pin, G. B. *J. Mol. Catal. A: Chem.* **2004**, *218*, 171–177.
(34) Shetti, V. N.; Rani, M. J.; Srinivas, D.; Ratnasamy, P. *J. Phys. Chem. B* **2006**, *110*, 677–679.

(35) Si, T. K.; Chakraborty, S.; Mukherjee, A. K.; Drew, M. G. B.; Bhattacharyya, R. *Polyhedron* **2008**, *27*, 2233–2242.
(36) Wei, X.; Ye, L.; Yuan, Y. *J. Nat. Gas Chem.* **2009**, *18*, 295–299.
(37) Borah, P.; Datta, A. *Appl. Catal., A* **2010**, *376*, 19–24.
(38) de Lima, S. M.; Gómez, J. A.; Barros, V. P.; Vertuan, G. de S.; das Dores Assis, M.; de Oliveira Graeff, C. F.; Demets, G. J.-F. *Polyhedron* **2010**, *29*, 3008–3013.
(39) Pokutsa, A.; Kubaj, Y.; Zaborovskyi, A.; Maksym, D.; Muzart, J.; Sobkowiak, A. *Appl. Catal., A* **2010**, *390*, 190–194.
(40) Si, T. K.; Chowdhury, K.; Mukherjee, M.; Bera, D. C.; Bhattacharyya, R. *J. Mol. Cat. A: Chem.* **2004**, *219*, 241–247.
(41) Reis, P. M.; Silva, J. A. L.; Fraústo da Silva, J. J. R.; Pombeiro, A. J. L. *J. Mol. Cat. A: Chem.* **2004**, *224*, 189–195.
(42) Zhang, J.; Tang, Y.; Li, G.; Hu, C. *Appl. Catal., A* **2005**, *278*, 251–261.
(43) Jian, M.; Zhu, L.; Wang, J.; Zhang, J.; Li, G.; Hu, C. *J. Mol. Cat. A: Chem.* **2006**, *253*, 1–7.
(44) Zhu, Y.; Dong, Y.; Zhao, L.; Yuan, F. *J. Mol. Cat. A: Chem.* **2010**, *315*, 205–212.
(45) Liu, Q.; Zhu, L.; Li, L.; Guo, B.; Hu, X.; Hu, C. *J. Mol. Catal. A: Chem.* **2010**, *331*, 71–77.
(46) Khatri, P. K.; Singh, B.; Jain, S. L.; Sain, B.; Sinha, A. K. *Chem. Commun.* **2011**, *47*, 1610–1612.
(47) Maurya, M. R.; Arya, A.; Adão, P.; Costa Pessoa, J. *Appl. Catal., A* **2008**, *351*, 239–252.
(48) Marchetti, C. F.; Pettinari, C.; Di Nicola, C.; Pettinari, R.; Crispini, A.; Crucianelli, M.; Di Giuseppe, A. *Appl. Catal., A* **2010**, *378*, 211–220.
(49) Hsiao, M.-C.; Liu, S.-T. *Catal. Lett.* **2010**, *139*, 61–66.
(50) Kirillova, M. V.; Kuznetsov, M. L.; Reis, P. M.; da Silva, J. A. L.; Fraústo da Silva, J. J. R.; Pombeiro, A. J. L. *J. Am. Chem. Soc.* **2007**, *129*, 10531–10545.
(51) Shul'pin, G. B.; Kozlov, Y. N. *Org. Biomol. Chem.* **2003**, *1*, 2303–2306.
(52) Shul'pin, G. B.; Attanasio, D.; Suber, L. *J. Catal.* **1993**, *142*, 147–152.
(53) Shul'pin, G. B.; Kozlov, Y. N.; Nizova, G. V.; Süss-Fink, G.; Stanislas, S.; Kitaygorodskiy, A.; Kulikova, V. S. *J. Chem. Soc., Perkin Trans. 2* **2001**, 1351–1371.
(54) Aboelfetoh, E. F.; Fechtelkord, M.; Pietschnig, R. *J. Mol. Catal. A: Chem.* **2010**, *318*, 51–59.
(55) de la Cruz, M. H. C.; Kozlov, Y. N.; Lachter, E. R.; Shul'pin, G. B. *New J. Chem.* **2003**, *27*, 634–638.
(56) Shul'pin, G. B.; Ishii, Y.; Sakaguchi, S.; Iwahama, T. *Russ. Chem. Bull.* **1999**, *48*, 887–890.
(57) Kozlov, Y. N.; Romakh, V. B.; Kitaygorodskiy, A.; Buglyó, P.; Süss-Fink, G.; Shul'pin, G. B. *J. Phys. Chem. A* **2007**, *111*, 7736–7752.
(58) Khaliullin, R. Z.; Bell, A. T.; Head-Gordon, M. *J. Phys. Chem. B* **2005**, *109*, 17984–17992.
(59) Kirillova, M. V.; Kuznetsov, M. L.; Romakh, V. B.; Shul'pina, L. S.; Fraústo da Silva, J. J. R.; Pombeiro, A. J. L.; Shul'pin, G. B. *J. Catal.* **2009**, *267*, 140–157.
(60) Shul'pin, G. B.; Drago, R. S.; Gonzalez, M. *Russ. Chem. Bull.* **1996**, *45*, 2386–2388.
(61) Romakh, V. B.; Süss-Fink, G.; Shul'pin, G. B. *Petrol. Chem.* **2008**, *48*, 440–443.
(62) Silva, T. F. S.; Alegria, E. C. B. A.; Martins, L. M. D. R. S.; Pombeiro, A. J. L. *Adv. Synth. Catal.* **2008**, *350*, 706–716.
(63) Shul'pina, L. S.; Kirillova, M. V.; Pombeiro, A. J. L.; Shul'pin, G. B. *Tetrahedron* **2009**, *65*, 2424–2429.
(64) Colpas, G. J.; Hamstra, B. J.; Kampf, J. W.; Pecoraro, V. L. *J. Am. Chem. Soc.* **1996**, *118*, 3469–3478.
(65) Zampella, G.; Fantucci, P.; Pecoraro, V. L.; De Gioia, L. *Inorg. Chem.* **2006**, *45*, 7133–7143.
(66) Schneider, C. J.; Zampella, G.; Greco, C.; Pecoraro, V. L.; De Gioia, L. *Eur. J. Inorg. Chem.* **2007**, 515–523.
(67) Schneider, C. J.; Penner-Hahn, J. E.; Pecoraro, V. L. *J. Am. Chem. Soc.* **2008**, *130*, 2712–2713.
(68) Bino, A.; Cohen, S.; Heitner-Wirguin, C. *Inorg. Chem.* **1982**, *21*, 429–431.
(69) Baxter, S. M.; Wolczanski, P. T. *Inorg. Chem.* **1989**, *28*, 3263–3264.
(70) Therrien, B.; Stanislas, S.; Stoeckli-Evans, H.; Shul'pin, G. B.; Süss-Fink, G. *Acta Crystallogr.* **2002**, *E58*, m215–m216.
(71) Slebodnick, C.; Pecoraro, V. L. *Inorg. Chim. Acta* **1998**, *283*, 37–43.
(72) Howarth, O. W.; Hunt, J. R. *J. Chem. Soc. Dalton* **1979**, 1388–1391.
(73) Harrison, A. T.; Howarth, O. W. *J. Chem. Soc. Dalton* **1985**, 1173–1177.
(74) Clague, M. J.; Butler, A. *J. Am. Chem. Soc.* **1995**, *117*, 3475–3484.
(75) Chrappová, J.; Schwendt, P.; Sivák, M.; Repiský, M.; Malkin, V. G.; Marek, J. *Dalton Trans.* **2009**, 465–473.
(76) Maurya, M. R.; Arya, A.; Kumar, A.; Kuznetsov, M. L.; Avecilla, F.; Costa Pessoa, J. *Inorg. Chem.* **2010**, *49*, 6586–6600.
(77) Tatiersky, J.; Schwendt, P.; Marek, J.; Sivák, M. *New. J. Chem.* **2004**, *28*, 127–133.
(78) Shul'pin, G. B.; Kozlov, Y. N.; Shul'pina, L. S.; Kudinov, A. R.; Mandelli, D. *Inorg. Chem.* **2009**, *48*, 10480–10482.
(79) Shul'pin, G. B.; Kozlov, Y. N.; Shul'pina, L. S.; Petrovskiy, P. V. *Appl. Organomet. Chem.* **2010**, *24*, 464–472.
(80) Süss-Fink, G.; Nizova, G. V.; Stanislas, S.; Shul'pin, G. B. *J. Mol. Catal. A: Chem.* **1998**, *130*, 163–170.
(81) Kozlov, Y. N.; Nizova, G. V.; Shul'pin, G. B. *J. Mol. Catal. A: Chem.* **2005**, *227*, 247–253.
(82) Shul'pin, G. B.; Nizova, G. V.; Kozlov, Y. N.; Gonzalez Cuervo, L.; Süss-Fink, G. *Adv. Synth. Catal.* **2004**, *346*, 317–332.
(83) Becke, A. D. *J. Chem. Phys.* **1993**, *98*, 5648–5652.
(84) Lee, C.; Yang, W.; Parr, R. G. *Phys. Rev.* **1988**, *B37*, 785–789.
(85) Frisch, M. J.; Trucks, G. W.; Schlegel, H. B.; Scuseria, G. E.; Robb, M. A.; Cheeseman, J. R.; Zakrzewski, V. G.; Montgomery, J. A., Jr.; Stratmann, R. E.; Burant, J. C.; Dapprich, S.; Millam, J. M.; Daniels, A. D.; Kudin, K. N.; Strain, M. C.; Farkas, O.; Tomasi, J.; Barone, V.; Cossi, M.; Cammi, R.; Mennucci, B.; Pomelli, C.; Adamo, C.; Clifford, S.; Ochterski, J.; Peterson, G. A.; Ayala, P. Y.; Cui, Q.; Morokuma, K.; Malick, D. K.; Rabuck, A. D.; Raghavachari, K.; Foresman, J. B.; Cioslowski, J.; Ortiz, J. V.; Baboul, A. G.; Stefanov, B. B.; Liu, G.; Liashenko, A.; Piskorz, P.; Komaromi, I.; Gomperts, R.; Martin, R. L.; Fox, D. J.; Keith, T.; Al-Laham, M. A.; Peng, C. Y.; Nanayakkara, A.; Challacombe, M.; Gill, P. M. W.; Johnson, B.; Chen, W.; Wong, M. W.; Andres, J. L.; Gonzalez, C.; Head-Gordon, M.; Replogle, E. S.; Pople, J. A. *Gaussian 98, revision A.9*; Gaussian, Inc.: Pittsburgh PA, 1998.
(86) Dolg, M.; Wedig, U.; Stoll, H.; Preuss, H. *J. Chem. Phys.* **1987**, *86*, 866–872.
(87) Tomasi, J.; Persico, M. *Chem. Rev.* **1997**, *94*, 2027–2094.
(88) Barone, V.; Cossi, M. *J. Phys. Chem.* **1998**, *102*, 1995–2001.
(89) Wertz, G. H. *J. Am. Chem. Soc.* **1980**, *102*, 5316–5322.
(90) Cooper, J.; Ziegler, T. *Inorg. Chem.* **2002**, *41*, 6614–6622.
(91) Reed, A. E.; Curtiss, L. A.; Weinhold, F. *Chem. Rev.* **1988**, *88*, 899.